Volume 12 | Issue 2 Article 12

Enhanced NO_2 Gas Sensing Using Silver-Doped Cadmium Telluride Nanocrystalline Thin Films

Tunis Balasim Hassan
Ministry of Education, Vocational Education Directorate, Baghdad, 10011, Iraq., Tunis20151@gmail.com

Recommended Citation

Hassan, Tunis Balasim (2026) "Enhanced NO_2 Gas Sensing Using Silver-Doped Cadmium Telluride Nanocrystalline Thin Films," *Karbala International Journal of Modern Science*: Vol. 12 : Iss. 2 , Article 12.
Available at: https://doi.org/10.33640/2405-609X.3450

Enhanced NO_2 Gas Sensing Using Silver-Doped Cadmium Telluride Nanocrystalline Thin Films

Abstract

Nitrogen dioxide (NO_2) is a toxic pollutant that necessitates sensitive and reliable monitoring systems. Conventional gas sensors often lack adequate responsiveness and fast recovery under changing conditions and therefore create a need for semiconductors with enhanced performance, especially at high industrial temperatures (around 250 °C). The study therefore aims to synthesis and evaluate silver-doped cadmium telluride (Ag:CdTe) thin films as NO_2 gas sensors. Pure CdTe and Ag:CdTe with silver concentrations of 5, 10, and 15 wt% were prepared by a co-precipitation process. XRD verified cubic symmetry with a progressive fall in crystallite size (6.67 nm to 5.46 nm at 15 wt% Ag), which increases grain-boundary density and the availability of surface-active sites and improves sensitivity and response speed. Field-emission scanning electron microscopy revealed uniform spherical nanoparticles with diameters of 20 to 30 nm that form porous networks favourable for gas adsorption. Optical analysis by UV–Vis spectroscopy showed a direct bandgap decrease from 1.85 to 1.6 eV as silver content increased, which corresponds to a red shift of the absorption edge and reflects Ag-induced tail states and refined crystallite domains that facilitate carrier generation under NO_2. Gas sensing tests were performed under 5% NO_2 at 6 V between 25 and 250°C. Sensitivity increased with temperature and reached 81.6% for 0.15 Ag:CdTe films at 250°C. The Ag:CdTe sensor showed a response time of 5.3 s and a recovery time of 28 s. The findings demonstrate that Ag:CdTe films synthesized by co-precipitation present an efficient NO_2 gas sensors for controlled ambient monitoring.

Keywords

NO2 gas; CdTe films; Ag-doping; Co-precipitation technique; Gas sensors.

RESEARCH PAPER

Enhanced NO_2 Gas Sensing Using Silver-doped Cadmium Telluride Nanocrystalline Thin Films

Tunis B. Hassan

Ministry of Education, Vocational Education Directorate, Baghdad, 10011, Iraq

Abstract

Nitrogen dioxide (NO_2) is a toxic pollutant that necessitates sensitive and reliable monitoring systems. Conventional gas sensors often lack adequate responsiveness and fast recovery under changing conditions and therefore create a need for semiconductors with enhanced performance, especially at high industrial temperatures (around 250 °C). The study therefore aims to synthesis and evaluate silver-doped cadmium telluride (Ag:CdTe) thin films as NO_2 gas sensors. Pure CdTe and Ag:CdTe with silver concentrations of 5, 10, and 15 wt% were prepared by a co-precipitation process. XRD verified cubic symmetry with a progressive fall in crystallite size (6.67 nm to 5.46 nm at 15 wt% Ag), which increases grain-boundary density and the availability of surface-active sites and improves sensitivity and response speed. Field-emission scanning electron microscopy revealed uniform spherical nanoparticles with diameters of 20 to 30 nm that form porous networks favourable for gas adsorption. Optical analysis by UV−Vis spectroscopy showed a direct bandgap decrease from 1.85 to 1.6 eV as silver content increased, which corresponds to a red shift of the absorption edge and reflects Ag-induced tail states and refined crystallite domains that facilitate carrier generation under NO_2. Gas sensing tests were performed under 5% NO_2 at 6 V between 25 and 250 °C. Sensitivity increased with temperature and reached 81.6% for 0.15 Ag:CdTe films at 250 °C. The Ag:CdTe sensor showed a response time of 5.3 s and a recovery time of 28 s. The findings demonstrate that Ag:CdTe films synthesized by co-precipitation present an efficient NO_2 gas sensors for controlled ambient monitoring.

Keywords: NO_2 gas, CdTe films, Ag-doping, Co-precipitation technique, Gas sensors

1. Introduction

Semiconductors, especially group II-VI semiconductors, have been used in different applications, including photovoltaic and photoconductive devices [1]. Heterojunctions (HJs) have gained extensive research attention over the past forty years because of their technological importance. When coal, gas, oil, or wood are burned for industrial or residential purposes, NO_2, a poisonous gas, is released. Vehicles with internal combustion engines are also major contributors. Concentrations above 200 $\mu g/m^3$ are harmful to human health and contribute to environmental problems such as acid rain [2,3]. Developing NO_2 monitoring systems that are highly sensitive, inexpensive, and stable at high temperatures is therefore essential.

CdTe is one of the remarkable II-VI compounds as it supports both p- and n-type conductivity. Among II-VI compounds, CdTe is widely used as an absorber in solar devices [4]. Its bandgap is around 1.5 eV and varies with doping concentration [5]. Thin films of CdTe have been fabricated using spray pyrolysis, close-space sublimation [6], reaction techniques, and vacuum evaporation [7]. Among these, close-space sublimation is often chosen due to its flexibility. CdTe also plays an essential role in laser heterostructures, thin film optical filters, infrared and ultraviolet detectors, photovoltaic cells, and field-effect transistors [8].

In addition to these optoelectronic applications, CdTe has recently been investigated for gas sensing. CdTe thin films demonstrated reversible ammonia sensing at room temperature with high

Received 1 September 2025; revised 19 December 2025; accepted 23 December 2025.
Available online 19 May 2026
E-mail address: tunis20151@gmail.com.

https://doi.org/10.33640/2405-609X.3450

sensitivity [9]. Hybrid CdTe/ZnO porous-silicon composites further improved NO_2 detection, showing around 19.8% response to 1 ppm NO_2 at 90 °C with fast response (13 s) and recovery (54 s), outperforming bare ZnO [10]. These results indicate that CdTe nanostructures can be tuned for enhanced gas sensing when combined with other semiconductors.

ZnO, SnO_2, In_2O_3, and other metal-oxide semiconductors remain widely studied NO_2 sensing materials. ZnO nanosheet films, for instance, reached sensitivities above 5000% for 100 ppm NO_2 at 150 °C, though with slower recovery [11]. Despite strong sensitivity, high operating temperatures and selectivity limitations constrain these oxides. Doping is frequently used to overcome such challenges. Silver (Ag) acts as an electronic and catalytic dopant, improving oxygen adsorption and modifying surface charge. Ag-doped In_2O_3 nanospheres showed a nearly 23-fold enhancement in NO_2 response at 62 °C compared to undoped films [12], while Ag-doped SnO_2 thin films displayed maximal sensitivity at around 3 mol% Ag before agglomeration reduced surface activity [13].

Ag doping in CdTe has also been shown to alter its structural, optical, and electronic characteristics across multiple applications. In Hg^{2+} detection studies, Ag-doped CdTe quantum dots with an average size of around 5 nm exhibited a high photoluminescence quantum yield of 59%, with multiple emission peaks appearing due to Ag-induced defect states [14]. In Ag-doped CdTe quantum dots synthesized via aqueous reflux, the Stokes shift decreased by around 120 meV, the fluorescence intensity increased by 3.5 times, and the radiative rate was enhanced by 4.2 times, all indicating reduced surface traps and improved recombination efficiency due to Ag incorporation [15]. Ag incorporation into polycrystalline reduced resistivity from 10^5 Ω·cm to 10^2 Ω·cm and increased hole concentration from 10^{14} to 10^{16} cm^{-3}, while mobility rose from 1.2 to 17 $cm^2 \cdot V^{-1} \cdot s^{-1}$ [16]. Quantitative shifts confirm that Ag^+ acts as a shallow acceptor, modifies the electronic band structure, and enhances charge transport. Ag-driven changes in band structure and charge transport are essential for optoelectronic efficiency and surface-mediated detection processes. The demonstrated tunability across structural scales and synthesis routes justifies further investigation of Ag:CdTe in gas sensing, where charge transfer and surface interaction dominate performance.

Beyond CdTe and doped oxides, emerging materials offer new possibilities. Graphene-based films achieved ultralow detection limits, with wearable graphene-oxide platforms detecting NO_2 at around 12.7 ppb [17]. Two-dimensional transition-metal dichalcogenides such as WS_2 exhibited layer-dependent sensitivity, with multilayers outperforming monolayers for NO_2 adsorption [18]. Halide perovskites have also been proposed, with mixed 2D/3D perovskite films providing rapid response (around 5.7 s), fast recovery (around 12.7 s), and long-term stability under ambient conditions [19]. Chemiresistive gas sensors offer direct two-terminal readout, low-cost thin-film fabrication, MEMS/CMOS compatibility, and real-time operation at elevated temperatures, which makes them well suited for NO_2 monitoring.

Although metal-oxide and two-dimensional materials dominate recent reports, evidence for NO_2 sensing at high temperatures (250 °C) remains limited. Prior studies seldom isolate the role of Ag loading or connect microstructural and optical changes to sensing behaviour at such temperatures. CdTe offers a promising balance of semiconducting properties, low-temperature synthesis compatibility, and tunability through silver doping. Therefore, the present work investigates Ag-doped CdTe films made by co-precipitation and aims to evaluate how silver incorporation affects their structural, optical, and sensing characteristics for NO_2 detection. The study thereby frames a structure-property-performance relationship for Ag:CdTe thin films operating at industrially relevant temperatures.

2. Materials and Methods

2.1. Materials

Tellurium dioxide (TeO_2, ≥99%), silver nitrate ($AgNO_3$, ≥99%), and cadmium acetate dihydrate [$Cd(CH_3COO)_2 \cdot 2H_2O$, ≥99%] were used as precursors. All solutions were prepared with double-distilled water to minimize ionic contamination.

2.2. Preparation of Ag-doped CdTe NPs

Cadmium telluride and silver-doped cadmium telluride (Ag:CdTe) films were synthesized by chemical co-precipitation. Three compositions of Ag:CdTe (5, 10, and 15 wt% Ag) were prepared. Initially, 50 mL of $Cd(CH_3COO)_2 \cdot 2H_2O$ solution and 50 mL of $AgNO_3$ solution (adjusted to the desired silver content) were mixed at 600 rpm at room temperature. Subsequently, 50 mL of TeO_2 solution was added dropwise to the cadmium-silver mixture to initiate precipitation. Stirring was continued for 2 h to ensure complete reaction and nucleation of Ag:CdTe nanoparticles. The resulting

dark gray precipitate was filtered and repeatedly washed with double-distilled water and methanol until free of soluble by-products. The precipitate was dried in air for 12 h and then ground using an agate mortar and pestle to obtain fine nanocrystalline powders.

2.3. Characterization methods

X-ray diffraction (Shimadzu, Japan) was used to investigate the crystalline structure and average crystallite size, which was estimated using Scherrer's equation. Field emission scanning electron microscopy (FESEM) was used to examine surface morphology and particle size distribution. Particle size was estimated from the FESEM images using ImageJ software (NIH, Bethesda, MD, USA). UV-Vis spectra (Jenway 6800, 200 to 1200 nm) were recorded to evaluate the effect of Ag incorporation on electronic transitions. The absorption coefficient was obtained from the absorbance data using the measured film thickness and optical path length. Film thickness was 150 nm across all samples and was used to compute the absorption coefficient.

2.4. Gas sensor testing system

A cylindrical steel chamber (diameter 163 mm, height 200 mm) with an O-ring-sealed removable base provided an effective volume of 4.173 L. The base included a multi-pin feedthrough for electrical connections to the sensor and heater assembly. The heater consisted of a hot plate and a K-type thermocouple, positioned to sense temperature at the film surface exposed to the analyte. The chamber featured three ports: an inlet for the test gas, an inlet valve for zero air after evacuation, and a port for a vacuum gauge. A rotary pump evacuated the chamber to 2×10^{-2} bar. A gas-mixing manifold with flow meter and needle-valve control premixed zero air with the test gas before injection into the chamber to ensure a stable and reproducible composition. Sensor conductance was recorded with a PC-interfaced multi-meter (UNI-T UT81B).

2.5. Gas sensing measurements

Gas sensing tests were conducted in a sealed test chamber equipped with a heating stage and thermocouple for temperature control. Thin film samples were deposited on alumina substrates with pre-patterned aluminium electrodes. A bias voltage of 6 V was applied across the electrodes. Sensitivity (S) was calculated from the change in resistance upon exposure to 5% NO_2 gas at operating temperatures between 25 and 250 °C, according to:

$$S = \left| \left(R_g - R_a\right) / R_a \right| \times 100\% \quad (1)$$

where R_g is the resistance in NO_2 and R_a is the baseline resistance in air. Response and recovery times were determined as the intervals required to reach 90% of the total resistance change upon gas exposure and removal, respectively.

Time-resolved conductance *G(t)* was recorded during step exposure to 5% NO_2 and subsequent purge with zero air at a fixed temperature and 6 V bias. A baseline G_0 was taken as the average over the final 30 s before NO_2 admission. A steady-state value G_{ss} was taken as the average over the final 30 s of the NO_2 plateau. The total change was $\Delta G = G_{ss} - G_0$. The response time was defined as the time required for *G(t)* to reach 90% of ΔG after valve opening; the recovery time was defined as the time required for *G(t)* to return to within 10% of G_0 after switching back to zero air. The same criteria were applied for all samples and temperatures.

Interpretation of temperature and Ag-content trends refers to the Langmuir isotherm and Langmuir-Hinshelwood surface scheme for coverage and reaction, Arrhenius kinetics for rate constants, and the Seto grain-boundary barrier model for polycrystalline transport.

3. Results and Discussion

3.1. Structure and morphology

The influence of silver incorporation on crystallinity, lattice order, and grain refinement plays a decisive role in determining the electronic behaviour and gas sensing performance of the Ag:CdTe films. Fig. 1 shows the XRD patterns of Ag:CdTe at various concentrations of Ag. The observed values of the peaks matched the standard CdTe JCPDS data (15-0770). It was found that each composition exhibited a cubic phase with (111), (220), and (311) reflections. The absence of a new phase in Ag doping indicates that neither the structure nor the composition changed upon the addition of silver to CdTe. It was evident that the Bragg peaks became stronger with increasing doping concentration. The crystalline peak intensities were highest at 0.10 Ag and decreased at 0.15 Ag. The enhancement in the crystalline quality of CdTe thin films with silver doping likely resulted from the introduction of additional nucleating centres by the doping atoms along with the optimal growth conditions for CdTe [20]. Using the Scherrer equation, the grain size was calculated [21].

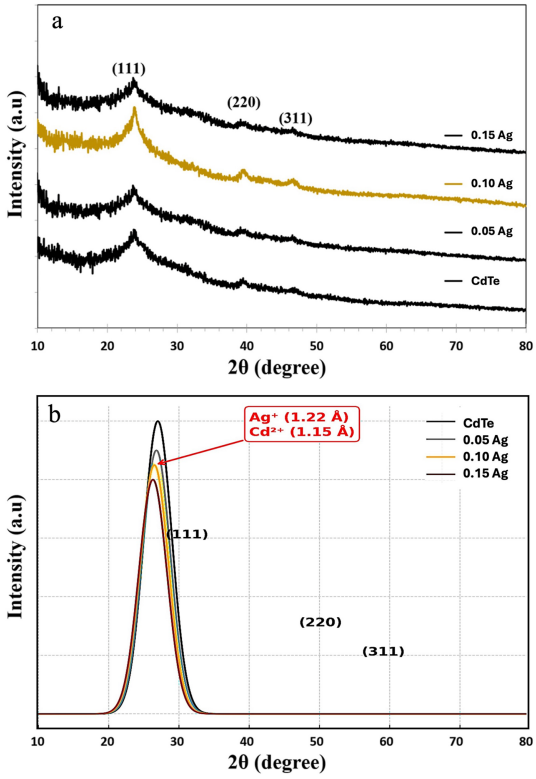

Fig. 1. X-ray diffraction pattern of CdTe and Ag:CdTe.

The films' crystalline quality declined despite the high doping concentration due to the freshly generated nucleating centres attained saturation and the ionic radius gap between Ag (1.22 Å) and Cd (1.15 Å) that increased lattice distortion. A higher Ag-ion content in Cd lattice planes increases lattice distortion and film strain, which disrupts normal crystal growth. In addition, the slight decrease in crystallite size with higher Ag:CdTe loading can also be associated with localized strain fields at the grain boundaries, which hinder crystal coalescence and lead to partial broadening of diffraction peaks. Such strain effects are common in heavily doped nanostructures and are often correlated with improved surface activity for catalytic and sensing processes.

The produced thin films' surface morphology was investigated using FESEM. Morphological images of the pure CdTe and Ag-doped CdTe thin films are shown (Fig. 2). The produced CdTe thin films were made from similar-sized spherical particles having a diameter of about (20-30) nm. Spherical nanoparticles were linked to the overall porous structure, which is useful for gas sensing applications because the efficacy of such sensors is largely dependent on nanostructure shapes and surface-to-volume ratios. The sensitivity toward target gases improved as a

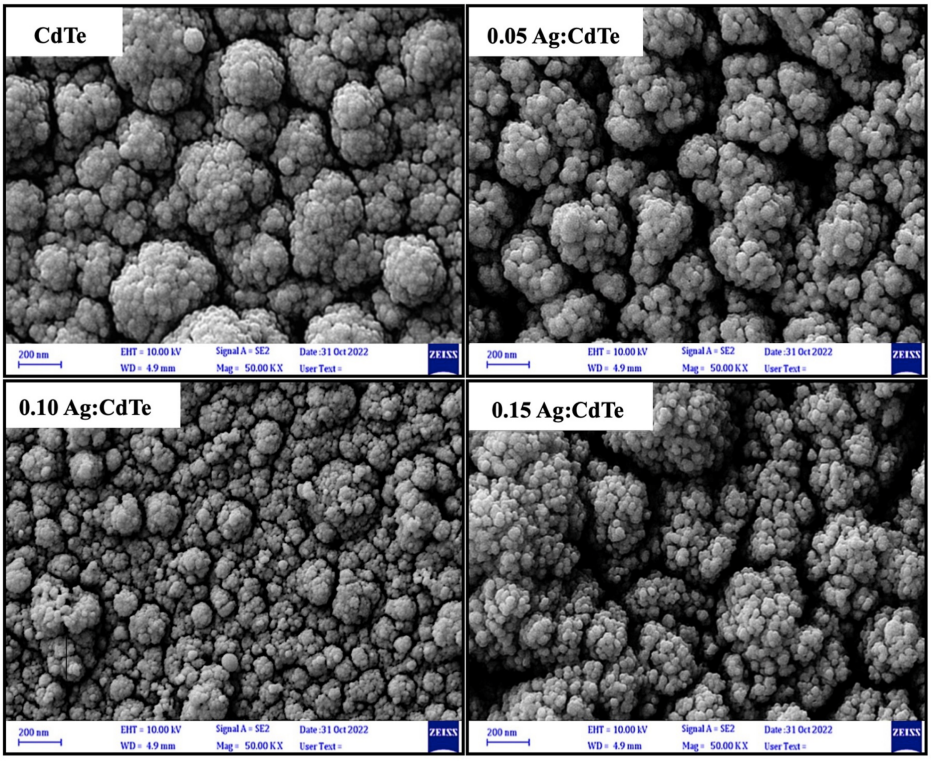

Fig. 2. FESEM image of CdTe and Ag:CdTe nanostructure at concentrations of 5, 10, and 15 wt%.

result of additional doping-induced changes in surface and interfacial characteristics, which enhanced gas adsorption. These characteristics offer multiple benefits for gas sensing applications, since the size, shape, and interconnectedness of neighbouring nanoparticles have a significant impact on sensor performance [22]. Furthermore, the porous network observed in Ag:CdTe films provides a larger number of adsorption sites compared to compact films, which directly contributes to improved sensitivity at high temperatures. The observed uniformity also confirms that the co-precipitation method yielded reproducible nanostructures with reliable morphology.

The average crystallite sizes of Ag:CdTe and undoped CdTe are listed in Table 1, which shows that crystallite size decreases as the Ag content increases. Such a trend highlights the importance of carefully optimizing Ag concentration to maximize crystallinity while avoiding excess strain.

XRD gave average crystallite sizes decreasing from 6.67 nm (CdTe) to 5.46 nm (0.15 Ag:CdTe). ImageJ analysis of FESEM micrographs yielded particle-size means of 102.97 ± 13.98 nm (CdTe), 113.23 ± 17.46 nm (0.05 Ag:CdTe), 122.54 ± 19.87 nm (0.10 Ag:CdTe), and 119.95 ± 15.39 nm (0.15 Ag:CdTe). The larger SEM values reflect agglomerates composed of multiple coherent domains; XRD probes coherent scattering lengths, whereas SEM resolves whole nanoparticles or clusters. The coexistence of nanometre-scale crystallites within around 100-120 nm particles increases grain-boundary area and active sites, which aligns with the higher sensitivity of Ag-doped films.

The particle size uniformity suggests that the doping process does not significantly alter the growth kinetics or morphology of the nanoparticles. The slight aggregation observed may result from van der Waals interactions or inadequate stabilization, which is typical in nanoparticle systems. The consistent particle size and shape are indicative of controlled synthesis conditions and ensure the reproducibility of nanostructures critical for their functional applications. Additionally, such morphological stability in Ag:CdTe systems implies that the primary role of Ag is electronic and catalytic rather than structural, which is advantageous for gas sensing where enhanced charge transfer and adsorption activity are desired.

Table 1. Average crystallite size for Ag-doped CdTe compared to undoped CdTe.

Sample	Concentration (wt%)	Crystallite size (nm)
CdTe	-	6.67015
Ag:CdTe	5	5.867092
Ag:CdTe	10	5.680831
Ag:CdTe	15	5.460382

3.2. Optical properties

The optical energy bandgap (*Eg*) was determined by applying the Tauc relation for direct bandgap semiconductors [16,23]:

$$(\alpha h\nu)2 = \beta\left(h\nu - Eg\right) \quad (2)$$

where α is the absorption coefficient, $h\nu$ is the photon energy, β is a proportionality constant, and *Eg* is the direct optical bandgap. The absorption coefficient was calculated from the absorbance data using film thickness and optical path length. Plots of $(\alpha h\nu)2$ versus $h\nu$ were constructed, and the bandgap was obtained by extrapolating the linear region of the curve to the energy axis. The method was selected because CdTe and Ag:CdTe films are direct semiconductors, and the Tauc relation provides an accurate determination of direct transition energies.

Optical bandgap and absorbance determine charge carrier generation, recombination, and transport in semiconductors, which directly govern sensing performance. Previous reports demonstrated that Ag incorporation into CdTe narrows the bandgap and red-shifts the absorption edge, thereby enhancing visible-light absorption and improving sensitivity in optoelectronic and sensing devices [24,25].

Fig. 3 presents the UV-Vis absorbance of CdTe and Ag:CdTe thin films over 300-1100 nm. Silver incorporation lowers the overall absorbance and produces an apparent blue shift of the high-slope region in the raw spectra. Band-edge positions were therefore determined from the absorption coefficient α using Tauc analysis for direct transitions, rather than by visual inspection of absorbance.

Fig. 4 reports a direct bandgap of 1.85 eV for undoped CdTe that decreases to 1.80, 1.75, and 1.60 eV for 5, 10, and 15 wt% Ag, respectively. The reduction indicates a shift to lower photon energy and aligns with Ag-induced tail states, increased defect density, and crystallite refinement that narrow the effective band structure.

3.3. Gas sensitivity characteristics

Since temperature has a significant impact on gas sensor functions, it is important to know the film sensitivity to determine its ideal operating temperature. In this investigation, the temperature was varied from 25 to 250 °C, and the applied voltage on

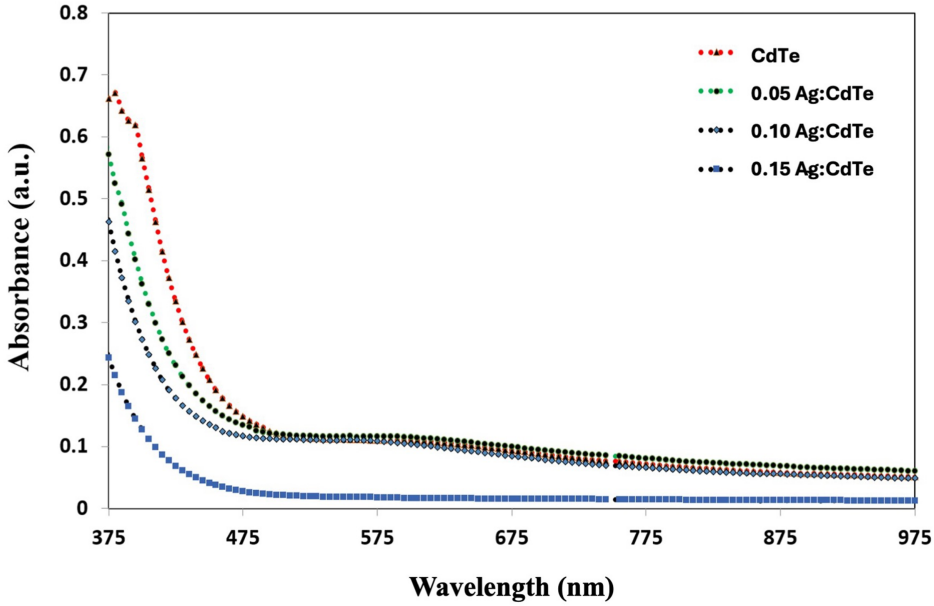

Fig. 3. Absorbance spectra of CdTe nanoparticles before and after Ag doping.

the electrodes was 6 V. The sensitivity value is calculated from equation (1) using 5% NO_2. Fig. 5 illustrates how the temperature affects the sensitivity of produced films. The results in Fig. 5 show how the sensitivity of pure and Ag:CdTe films changes (5, 10, 15 wt%), demonstrating that at 25 °C the sensitivity value for Ag:CdTe films is marginally higher than that of pure films (sensitivities are CdTe: 15%, 0.05 Ag:CdTe: 21%, 0.10 Ag:CdTe: 23%, 0.15 Ag:CdTe: 25%). Such sensitivity difference is due to the doping-induced decrease in grain size and the increase in surface area of the films, rather

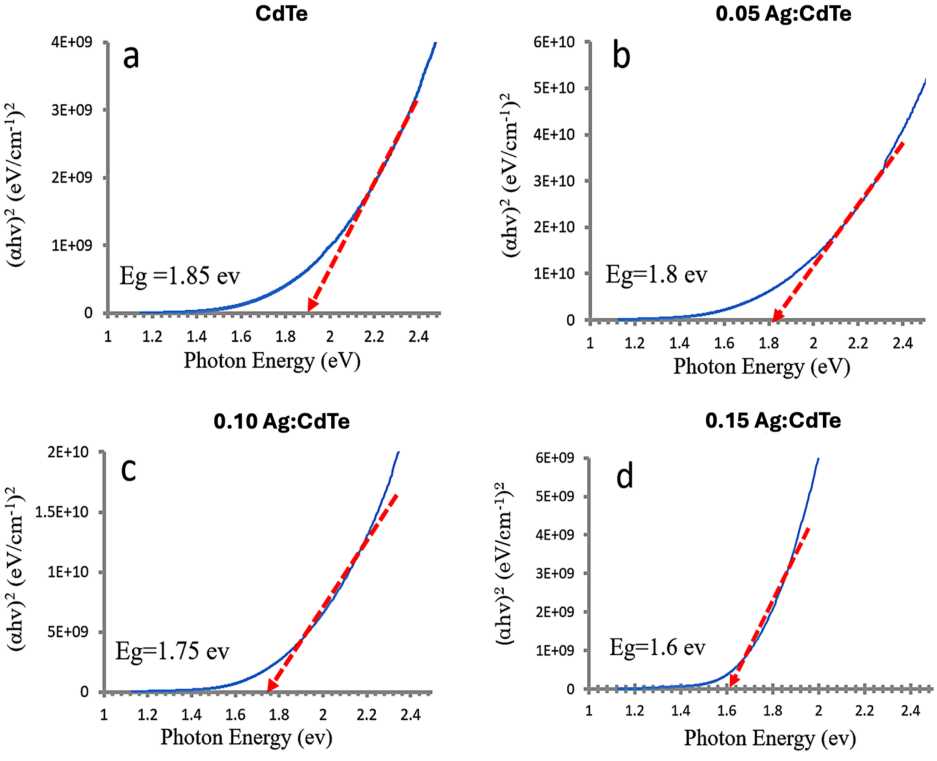

Fig. 4. Energy band gap variation of CdTe nanoparticles before and after Ag doping.

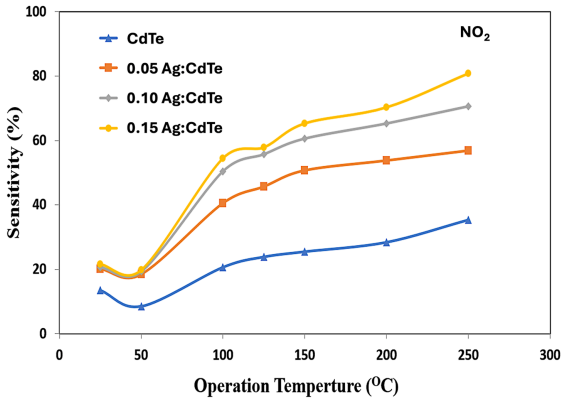

Fig. 5. The sensitivity of the prepared CdTe films varies with temperature.

than strong interactions between gas molecules and doped material, since adsorption at this stage corresponds to physisorption. However, when the temperature rises to 50 °C, the sensitivity falls, and the decrease is greater for pure films. Such reduction is attributed to an increase in electrical resistance on the semiconductor surface, which occurs as oxygen interacts with the film [26]. The adsorption process changes from physical to chemical and leads to the formation of an oxygen layer chemically bound to the oxide surface. The adsorbed layer withdraws electrons from the semiconductor surface, which increases the depletion width and raises sensor resistance. Several pathways describe oxygen interaction with the sensor surface [26]:

$$O_2(\text{gas}) \rightarrow O_2(\text{phys}) \rightarrow O_2^-(\text{chem}) \rightarrow 2O^-(\text{chem}) \rightarrow 2O^{2-}(\text{chem})$$

At approximately 50 °C, equilibrium forms between CdTe and atmospheric oxygen, and the conductivity value stabilizes. Higher temperatures enable NO_2 molecules to interact with the chemisorbed oxygen or directly capture electrons from the CdTe surface. The reactions can be represented as:

$$NO_2(\text{gas}) + e^- \rightarrow NO_2^-(\text{ads})$$

$$NO_2(\text{gas}) + O_2^-(\text{ads}) + e^- \rightarrow NO + 2O^-(\text{ads})$$

These interactions extract electrons from the conduction band and expand the depletion region, which leads to an increase in film resistance under NO_2 exposure. The extent of this resistance change determines the sensitivity of the Ag-doped CdTe film. For doped films, the sensitivity value is consistently greater than that of pure films (ranging from double to threefold higher, Fig. 5). The sensitivity profiles indicate that the peak response of both pure and Ag doped films occurs between 125 and 150 °C, a range attributed to the gas interaction mechanism at the sensor surface. Two factors govern the sensor response [27]. The first is the rapid chemical reaction occurring at the grain surface. The second is the diffusion velocity of NO_2 molecules into the oxide surface. At lower temperatures, response is controlled by fast surface reactions, whereas at higher temperatures, gas diffusion velocity becomes the determining factor. At intermediate temperatures, both processes contribute simultaneously [28].

Fig. 6a shows how response time changes with Ag doping percentage. The response time decreases as doping concentration increases. At 0.10 Ag:CdTe, a fast response time of 5.4 s was observed, accompanied by a recovery time of 25.2 s. Fig. 6b shows that recovery time decreases in proportion to doping level. Doping at 0.10 Ag had no significant influence on recovery time, which indicates that the fundamental gas-film interaction mechanism remained unchanged at this composition. Recovery time was also minimal, and the changes observed between 0.05 and 0.10 Ag doped films indicated strong gas-film interactions, as reported elsewhere [29].

Ag:CdTe exhibits higher response than undoped CdTe because Ag serves as a shallow acceptor that increases hole density and strengthens band bending under NO_2, and Ag sites catalyse oxygen/NO_2 adsorption and enable spillover, which raises surface coverage and reaction rates. Ag incorporation refines crystallites and promotes a porous

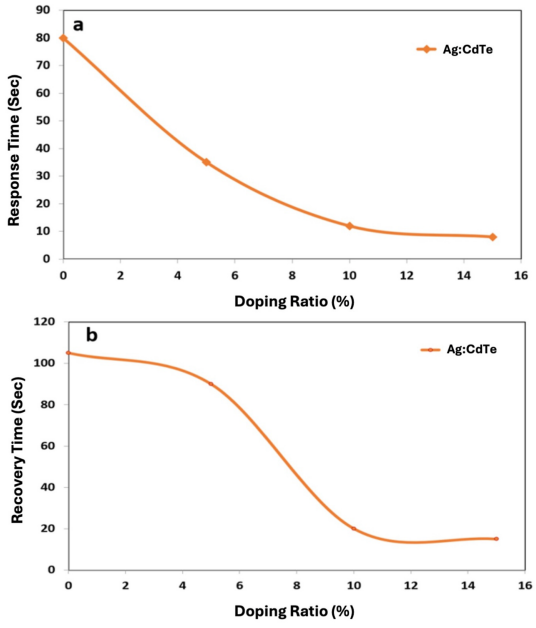

Fig. 6. Response time (a); Recovery time (b) for Ag:CdTe.

network, which increases grain-boundary area and the number of active sites and amplifies intergranular barrier modulation. The combined electronic, catalytic, and microstructural effects produce larger conductance changes and faster kinetics than CdTe.

Direct investigations of Ag-doped CdTe sensors are scarce, yet related CdTe-based hybrids demonstrate consistent improvements in NO_2 detection. An Ag-CdS coated optical fibre sensor reached 15.5% sensitivity at 100 ppm NO_2, which was significantly higher than the response of a comparable undoped CdS film [30]. In the case of CdTe/ZnO composites supported on porous Si, the reported NO_2 sensitivity was approximately 19.8% at 90 °C [10], while CdTe quantum-dot functionalised MoS_2 films exhibited about 40% sensitivity at room temperature [31]. By comparison, our results indicate that Ag incorporation into CdTe produces an enhancement in sensitivity that is roughly three- to fourfold greater, with faster kinetics, than values reported for previously studied CdTe-based nanostructures.

4. Conclusion

CdTe and Ag:CdTe thin films were successfully synthesized by the co-precipitation method and evaluated for their structural, optical, and gas sensing properties. XRD results confirmed the cubic crystalline phase of CdTe, with no secondary phases after Ag incorporation. Moderate doping levels enhanced crystallinity, while higher concentrations introduced lattice strain and reduced average crystallite size. FESEM images revealed uniform spherical nanoparticles with interconnected porous networks, features that are highly beneficial for gas adsorption. Optical analysis showed that Ag doping caused a red shift in the absorption edge and a progressive narrowing of the direct bandgap from 1.85 eV in pure CdTe to 1.6 eV at 0.15 Ag. Ag-induced bandgap reduction increases charge-carrier generation and accelerates electron transfer, and both effects support stronger gas-sensing performance. Gas-sensing measurements showed higher NO_2 sensitivity for Ag:CdTe films than for undoped CdTe at all tested temperatures. Peak sensitivity reached 81.6% at 250 °C for 0.15 Ag:CdTe (15 wt% Ag), with a response time of 5.3 s and a recovery time of 28 s. A porous nanoparticle network increases accessible surface area and improves gas diffusion, while Ag sites provide catalytic centres that promote NO_2 surface reactions. Ag:CdTe thin films therefore represent promising candidates for high-performance NO_2 sensing at high operating temperatures. Tuneable bandgap, higher sensitivity, and faster response kinetics support deployment in high-temperature ambient monitoring. Future work may optimise Ag concentration, evaluate stability under different humidity levels, and integrate the films into practical sensing devices.

Ethics information

Ethical approval was not required for this study because the work did not involve human participants, human data, animals, or animal-derived samples.

Funding

This work received no funding.

Conflict of interest

The author declares that they have no competing interests.

Acknowledgements

We deeply thank PHi NanoScience Center (PNSC, https://phi-nano.com) for supporting this work.

References

[1] S. Chander, M.S. Dhaka, Optimization of physical properties of vacuum evaporated CdTe thin films with the application of thermal treatment for solar cells, Mater. Sci. Semicond. Process. 40 (2015) 708–712, https://doi.org/10.1016/j.mssp.2015.07.063.
[2] D. Gu, X. Li, Y. Zhao, J. Wang, Enhanced NO_2 sensing of SnO_2/SnS_2 heterojunction based sensor, Sensor. Actuator. B Chem. 244 (2017) 67–76, https://doi.org/10.1016/j.snb.2016.12.125.
[3] J. Zhang, J. Wu, X. Wang, D. Zeng, C. Xie, Enhancing room-temperature NO_2 sensing properties via forming heterojunction for NiO-rGO composited with SnO_2 nanoplates, Sensor. Actuator. B Chem. 243 (2017) 1010–1019, https://doi.org/10.1016/j.snb.2016.12.062.
[4] A. Romeo, E. Artegiani, CdTe-Based thin film solar cells: past, present and future, Energies 14 (2021) 1684, https://doi.org/10.3390/en14061684.
[5] H.J. Scheel, T. Fukuda, Crystal Growth Technology, John Wiley & Sons, Ltd., Hoboken. 2003, https://doi.org/10.1002/0470871687.
[6] I.H. Khudayer, B.H. Hussein, M. Hamid, Depending the structure and optical properties of cadmium telluride films on the doping process, Al-Mustansiriyah J. Sci. 29 (2018) 160–167, https://doi.org/10.23851/mjs.v29i1.259.
[7] H.S. Patel, J.R. Rathod, K.D. Patel, V.M. Pathak, Structural and surface studies of vacuum evaporated cadmium telluride thin films, Am. J. Mater. Sci. Technol. 1 (2012) 11–17, https://doi.org/10.7726/ajmst.2012.1003.
[8] A. Hussain, A. Begum, A. Rahman, Electrical and optical properties of nanocrystalline lead sulphide thin films prepared by chemical bath deposition, Indian J. Phys. 86 (2012) 697–701, https://doi.org/10.1007/s12648-012-0130-2.

[9] J. Strobel, L. Ghimpu, V. Postica, O. Lupan, M. Zapf, S. Schönherr, R. Röder, C. Ronning, F. Schütt, Y.K. Mishra, I. Tiginyanu, R. Adelung, J. Marx, B. Fiedler, L. Kienle, Improving gas sensing by CdTe decoration of individual aerographite microtubes, Nanotechnology 30 (2019) 065501, https://doi.org/10.1088/1361-6528/aaf0e7.
[10] J. Jaiswal, P. Singh, R. Chandra, Low-Temperature Highly Selective and Sensitive NO_2 Gas Sensors Using CdTe-Functionalized ZnO Filled Porous Si Hybrid Hierarchical Nanostructured Thin Films, Sensor. Actuator. B Chem. 327 (2021) 128862, https://doi.org/10.1016/j.snb.2020.128862.
[11] M.A. Belal, S. Hajra, S. Panda, K.R. Kaja, K.J. Park, H.J. Kim, Spray-printed ZnO thin film for high-sensitivity NO_2 gas sensing, Micro Nano Syst. Lett. 13 (2025) 10, https://doi.org/10.1186/s40486-025-00230-8.
[12] M. Ding, N. Xie, C. Wang, X. Kou, H. Zhang, L. Guo, Y. Sun, X. Chuai, Y. Gao, F. Liu, Enhanced NO_2 gas sensing properties by Ag-Doped hollow urchin-like In_2O_3 hierarchical nanostructures, Sensor. Actuator. B Chem. 252 (2017) 418–427, https://doi.org/10.1016/j.snb.2017.06.016.
[13] P.S. Kolhe, P.M. Koinkar, N. Maiti, K.M. Sonawane, Synthesis of Ag doped SnO_2 thin films for the evaluation of H_2S gas sensing properties, Phys. B Condens. Matter 524 (2017) 90–96, https://doi.org/10.1016/j.physb.2017.07.056.
[14] H. Li, W. Lu, G. Zhao, B. Song, J. Zhou, W. Dong, G. Han, Silver ion-doped CdTe quantum dots as fluorescent probe for Hg^{2+} detection, RSC Adv. 10 (2020) 38965–38973, https://doi.org/10.1039/D0RA07140D.
[15] S.J. Ding, S. Liang, F. Nan, X.L. Liu, J.H. Wang, L. Zhou, X.F. Yu, Z.H. Hao, Q.Q. Wang, Synthesis and enhanced fluorescence of Ag-Doped CdTe semiconductor quantum dots, Nanoscale 7 (2015) 1970–1976, https://doi.org/10.1039/C4NR05731G.
[16] N.A. Shah, A. Ali, A.K.S. Aqili, A. Maqsood, Physical properties of Ag-Doped cadmium telluride thin films fabricated by closed-space sublimation technique, J. Cryst. Growth 290 (2006) 452–458, https://doi.org/10.1016/j.jcrysgro.2006.01.051.
[17] J. Khan, V. Rezo, T. Vincze, M. Weis, S.A. Momin, N. El-Atab, M. Jaafar, Flexible and highly selective NO_2 gas sensor based on direct-ink-writing of eco-friendly graphene oxide for smart wearable application, Chemosphere 367 (2024) 143618, https://doi.org/10.1016/j.chemosphere.2024.143618.
[18] Y. Zhou, S. Wang, S. Xin, S. Sayin, Z. Yi, Z. Li, M. Zaghloul, Layer-dependent sensing performance of WS_2-Based gas sensors, Nanomaterials 14 (2024) 235, https://doi.org/10.3390/nano14020235.
[19] A.T. John, H. Chen, H. Pham, K. Murugappan, T. Tran-Phu, A. Tricoli, K. Catchpole, Mixed-dimensional Organic-Inorganic Metal Halide Perovskite (OIMHP) based gas sensors with superior stability for NO_2 detection, Mater. Adv. 3 (2022) 1263–1271, https://doi.org/10.1039/D1MA00976A.
[20] Z.R. Khan, M. Zulfequar, M.S. Khan, Structural, optical, photoluminescence, dielectric and electrical studies of vacuum-evaporated CdTe thin films, Bull. Mater. Sci. 35 (2012) 169–174, https://doi.org/10.1007/s12034-012-0274-x.
[21] T.B. Hassan, S.M. Salih, Affect various capping agents on structural and optical properties of ZnS nanoparticles by Co-Precipitation method, in: AIP Conf. Proc., AIP Publishing LLC. 2022 020188, https://doi.org/10.1063/5.0093188.
[22] H.N. Noori, A.F. Abdulameer, Study of optical and structural properties of CdTe quantum dots capped with 3MPA using hydrothermal method, Chem. Methodol. 6 (2022) 842–850, https://doi.org/10.22034/CHEMM.2022.353494.1583.
[23] G.H. Tariq, M. Anis-ur-Rehman, Annealing effects on physical properties of doped CdTe thin films for photovoltaic applications, Mater. Sci. Semicond. Process. 30 (2015) 665–671, https://doi.org/10.1016/j.mssp.2014.09.012.
[24] A. Hazem, A. Adyan, M.H. Mustafa, Influence of silver doping on the properties of sprayed cadmium telluride films, J. Phys.: Conf. Ser. 3028 (2025) 012048, https://doi.org/10.1088/1742-6596/3028/1/012048.
[25] H. Wang, L. Zhang, C. Ding, M. Ali, H. Qi, F. Wang, G. Wang, W. Sun, Ultrafast nonlinear optical properties of Ag-CdTe thin films by Co-Sputtering in the near-infrared region, Opt. Mater. 142 (2023) 114062, https://doi.org/10.1016/j.optmat.2023.114062.
[26] R.S. Alnaily, M.L. Sheqnab, Study the optical and structure properties of CdTe nanoparticles prepared by pulsing laser ablation in distilled water, J. Kufa-Phys. 11 (2019) 82–89, https://doi.org/10.31257/2018/JKP/2019/110111.
[27] R.H. Bari, S.B. Patil, A.R. Bari, Synthesis, characterization and gas sensing performance of sol-gel prepared nanocrystalline SnO_2 thin films, Int. J. Smart Sens. Intell. Syst. 7 (2014) 610–629, https://doi.org/10.21307/ijssis-2017-672.
[28] S. Basu, Y.-H. Wang, C. Ghanshyam, P. Kapur, Fast response time alcohol gas sensor using nanocrystalline F-Doped SnO_2 films derived via sol-gel method, Bull. Mater. Sci. 36 (2013) 521–533, https://doi.org/10.1007/s12034-013-0493-9.
[29] S. Navale, M. Shahbaz, A. Mirzaei, S.S. Kim, H.W. Kim, Effect of Ag addition on the gas-sensing properties of nanostructured resistive-based gas sensors: an overview, Sensors 21 (2021) 6454, https://doi.org/10.3390/s21196454.
[30] A.K.C. Theoderaj, I.D. Jacob, M. Chitra, Ag-CdS-Coated cladding-modified fiber-optic sensor for detection of NO_2 gas, Nano 20 (2025) 2450106, https://doi.org/10.1142/S1793292024501066.
[31] J. Jaiswal, A. Sanger, P. Tiwari, R. Chandra, MoS2 hybrid heterostructure thin film decorated with CdTe quantum dots for room temperature NO_2 gas sensor, Sensor. Actuator. B Chem. 305 (2020) 127437, https://doi.org/10.1016/j.snb.2019.127437.